第 50 卷 第 21 期/2023 年 11 月/中国激光 研究论文

中国激光

# 腹腔镜用液体透镜变焦光学系统设计研究

董健，王春艳*，孙昊，刘欢，滕云杰

长春理工大学光电工程学院，吉林 长春 130022

**摘要** 针对传统变焦腹腔镜调焦结构所需空间大、调焦精度难以保证等问题，提出了一种以液体透镜为核心元件参与变焦的腹腔镜光学系统，利用液体透镜代替机械变焦结构，实现了变焦功能。推导了液体透镜电压与焦距的关系方程，结合COMSOL软件设计并仿真了满足所需焦距范围的双液体透镜。用ZEMAX软件设计优化了腹腔镜液体透镜变焦光学系统，通过控制电压即可实现焦距5～15 mm范围内同一像面高清晰成像。在焦距15 mm时，全视场点列图均方根（RMS）半径为6.694 μm，在焦距5 mm时，全视场点列图RMS半径为4.596 μm，均小于7.4 μm的像元尺寸。系统调制传递函数（MTF）在68 lp/mm处均大于0.5，4个组态（焦距分别为5、7.2、10.4、15 mm）畸变分别为7.047%、1.961%、0.732%、0.295%，满足腹腔镜对光学系统畸变的要求。

**关键词** 光学设计；变焦系统；液体透镜；腹腔镜；COMSOL；ZEMAX

**中图分类号** O435 **文献标志码** A **DOI：** 10.3788/CJL231015

## 1 引 言

无创和微创治疗已成为外科手术的主要途径，内窥镜在其中起到了不可替代的作用。医用内窥镜多为细长结构，便于伸入体内。目前医用内窥镜主要采用定焦光学系统，依靠图像处理等手段进行图片缩放。传统机械变焦方式由于机械结构所占空间大、变焦困难等问题，目前还没有应用到医用内窥镜中。若将变焦距光学系统应用于内窥镜中，可以在保证视场不变的情况下在更深范围内搜索病变组织，实现一定深度区域病灶的清晰放大，亦可在同一深度实现更小病变组织的放大，使用者无需处理图像即可实现微小病灶的观察。

液体透镜基于仿生学概念提出，是一种体积小、可集成、拥有自主变焦能力的新型透镜，随着电润湿迟滞[1-2]、接触角饱和[3-5]等现象的相继发现和研究的不断深入，电润湿型液体透镜技术日益成熟。将电润湿型液体透镜应用于医用内窥镜设计中，仅通过调节电压便可实现变焦成像，同时保证成像质量。

国内外已经有学者对含液体透镜的内窥镜光学系统展开了研究[6-7]。2010年，Tsai等[8]提出腹腔镜摄像机的构想，设计以液体透镜调焦的腹腔镜变焦相机，并在活猪身上进行了测试，效果不错；2013年，韩国实验室设计了四倍变焦腹腔镜系统，焦距范围3.24～12.95 mm，最大畸变值16%，系统利用单液体透镜进行调焦时需要电机控制，影响了系统的结构紧凑性[9]；2015年，郭鑫等[10]提出了一种新型单液体电控型液体透镜，设计出了液体透镜调焦胶囊内窥镜光学系统，视场角达110°以上，景深范围3～100 mm，系统最大畸变值为35.54%。然而，难以在获得高清晰图像的同时满足畸变小、结构紧凑要求的问题还有待进一步解决。本文针对医用腹腔镜使用需求，以传统变焦光学系统理论为基础，使用电润湿型液体透镜代替变倍组、补偿组，设计了一款基于液体透镜的腹腔镜用变焦光学系统。设计结果表明，系统在无机械结构参与变焦的情况下，可实现焦距范围在5～15 mm内的清晰成像，最大畸变存在于焦距最短时，为7.047%，优于查到的公开发表文献[9]中最大畸变为16%的指标。

## 2 液体透镜变焦原理

本文选择电润湿型[11-14]液体透镜为核心变焦元件，仅靠调节电压就可改变界面曲率，同时电润湿型液体透镜也更便于小型化，精密程度高，符合设计需求。图1为圆柱形双液体透镜结构示意图，图中$D$为液体透镜口径，$d$为疏水层厚度，$n_1$、$n_2$为两种液体的折射率，$v_1$、$v_2$为两种液体的阿贝数，$r$为液体界面的半径。圆柱管材料为金属钢，圆柱壁内侧涂有疏水层[15]，疏水层采用疏水性介质Teflon制作。在圆柱管内注入等体积的两种不相溶透明液体，其中，液体腔1为导电溶液（NaCl），液体腔2为绝缘非极性液体（硅油），两种液体密度相同，可使双液体透镜中间界面为球面且稳定性高。在侧壁施加电压$U$，通过调节电压实现接触角$\theta$

**收稿日期**：2023-07-12；**修回日期**：2023-08-01；**录用日期**：2023-08-18；**网络首发日期**：2023-09-15

**基金项目**：吉林省教育厅科学技术研究项目（JJKH20220755KJ）、吉林省科技发展计划（20220201074GX）

**通信作者**：*245044961@qq.com

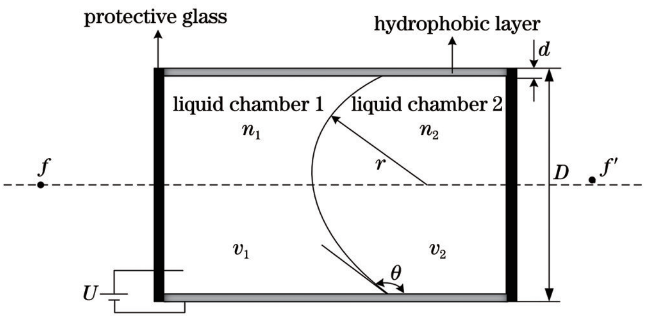


图 1 电润湿液体透镜结构示意图

Fig. 1 Structure diagram of electrowetting liquid lens

的变化，从而改变半径 $r$，实现焦距的变化。

双液体透镜焦距 $f$ 为[16]

$$f=\frac{r}{n_2-n_1}。\tag{1}$$

电润湿型液体透镜的焦距与外加电压有关。电润湿效应的物理机制可以归结为 Lippman-Young 方程[17]：

$$\cos\theta=\cos\theta_0+\frac{\varepsilon\varepsilon_0}{2\gamma_{12}d}U^2,\tag{2}$$

式中：$\theta_0$ 为初始接触角；$\varepsilon$ 为介电层相对介电常数；$\varepsilon_0$ 为真空的相对介电系数；$\gamma_{12}$ 为界面张力。

考虑到几何关系

$$r=-\frac{D}{2\cos\theta},\tag{3}$$

根据式（1）～式（3）得该双液体透镜的焦距为

$$f=\frac{D}{2(n_1-n_2)\cos\theta_0+\frac{\varepsilon_0\varepsilon_r(n_1-n_2)}{d\gamma_{12}}U^2},\tag{4}$$

式中：$\varepsilon_r$ 为疏水层介质材料的相对介电系数。

由式（4）可知，改变电压即可改变液体透镜的焦距。

# 3 变焦光学系统设计

## 3.1 设计指标

对医用腹腔镜光学系统，需要根据相关技术指标确定光学系统基本参数，主要包括：焦距、视场角、相对孔径、工作波长、点列图均方根（RMS）值、畸变量以及在截止频率时的调制传递函数（MTF）值。具体指标要求如表 1 所示。选用 1/3 英寸（1 英寸≈2.54 cm）电荷耦合器件（CCD）传感器，其对角线长 6 mm，像元尺寸 7.4 μm×7.4 μm，截止频率为 68 lp/mm。除长焦 15 mm、短焦 5 mm 外，再选取中间两个位置焦距进行分析。中间位置选取方法按下式实施：

$$5q^3=15,\tag{5}$$

式中：$q$ 为比例因子，经计算得 $q$=1.44。

由式（5）算得中间两组态焦距为 7.2 mm 和 10.4 mm。

表 1 腹腔镜用变焦光学系统指标要求

Table 1 Index requirements of laparoscopic zoom optical system

| Parameter | Value |
|---|---|
| Wavelength coverage /nm | 486–656 |
| Zoom part system caliber /mm | ≤6.2 |
| System outside diameter /mm | ≤10 |
| Overall length /mm | ≤45 |
| Focal length /mm | 5–15 |
| Field angle range /(°) | 24–64 |
| MTF /(lp·mm$^{-1}$) | ≥0.3 |
| Optical distortion /% | <15 |

## 3.2 机械变焦结构初始结构设计

传统变焦光学系统要求在焦距 $f$ 或者倍率 $m$ 变化时系统共轭距不变，且在变焦过程中成像质量不变。传统变焦系统组成如图 2 所示。其中，补偿组根据变倍组的移动做出相应的补偿[18]。

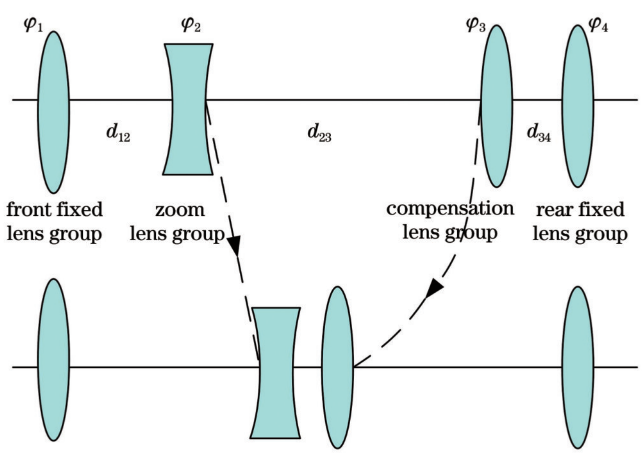


图 2 系统结构组成

Fig. 2 System structure composition

设计思路为：根据表 1 给出的指标要求，确定初始结构，在 ZEMAX 软件中加入操作数进行优化。需控制变倍组和补偿组口径在 6 mm 左右，留出机械结构设计余量，最终得到变焦腹腔镜光学初始结构如图 3 所示。

## 3.3 液体透镜设计仿真

本文采用电润湿型液体透镜来代替图 3 变焦系统的变倍组与补偿组，以达到无机械结构调焦的目的。应用 COMSOL 软件[19-20]对所需的电润湿液体透镜进行仿真，选用流体流动模块的层流两相流网格构建液体透镜界面的清晰模型。

根据图 3 焦距变化范围和光学系统口径确定液体透镜参数。口径 $D$ 为 6 mm，疏水层厚度 $d$ 为 1.5 μm，圆柱体高（即液体总厚度）2 mm，液体 1 的折射率 $n_1$＝1.33，色散系数 $v_1$＝54.6，液体 2 的折射率 $n_2$＝1.65，色散系数 $v_2$＝44.8，通过仿真分析最终得出液体透镜

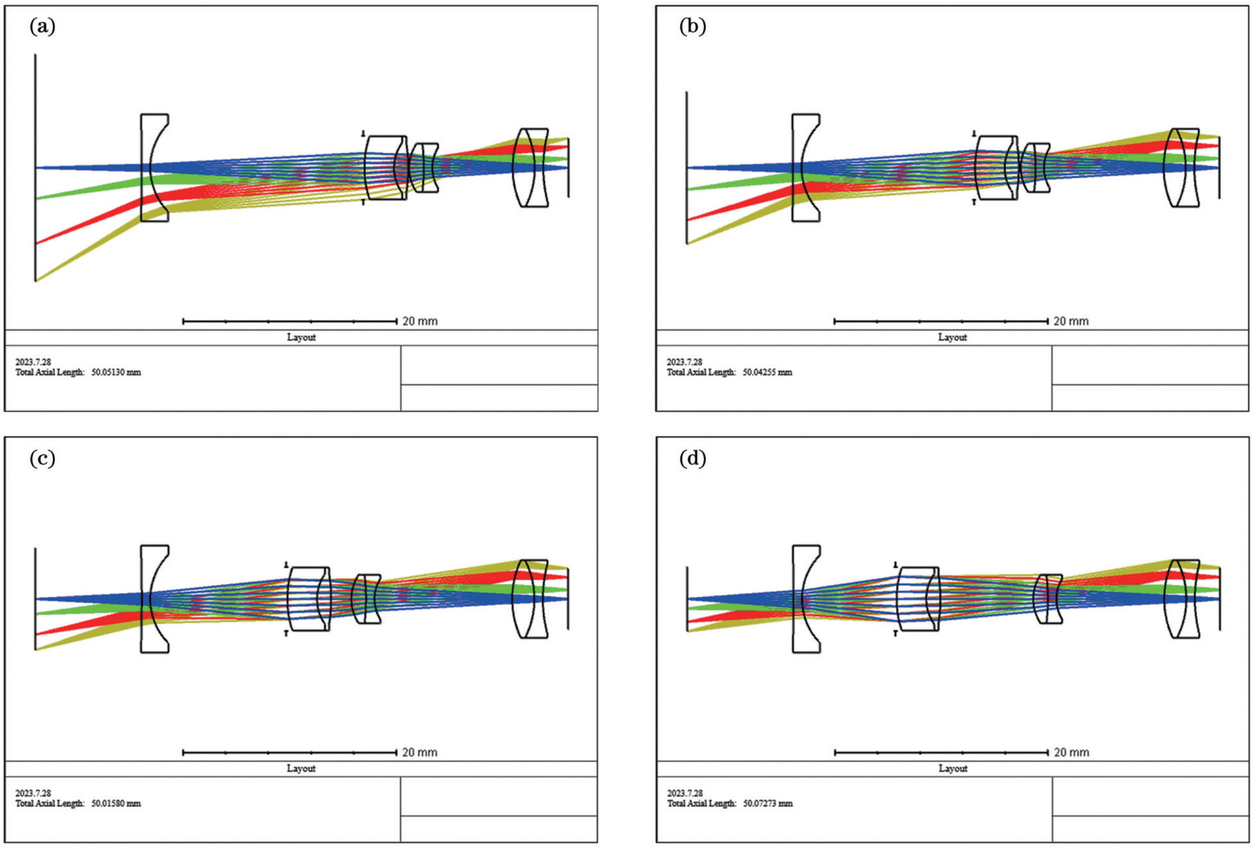


图3 机械变焦系统结构图。(a)焦距5 mm;(b)焦距7.2 mm;(c)焦距10.4 mm;(d)焦距15 mm

Fig. 3 Structure diagram of mechanical zoom system. (a) Effective focal length (EFL) 5 mm; (b) EFL 7.2 mm; (c) EFL 10.4 mm; (d) EFL 15 mm

焦距范围(−∞, −7.79 mm ]∪[ 18 mm, +∞)。

图4分别为电压0、35、60 V时液体透镜界面的仿真图，不同颜色表示不同的流速，箭头表示液体流动方向。从图中可以明显看到当电压逐渐增加

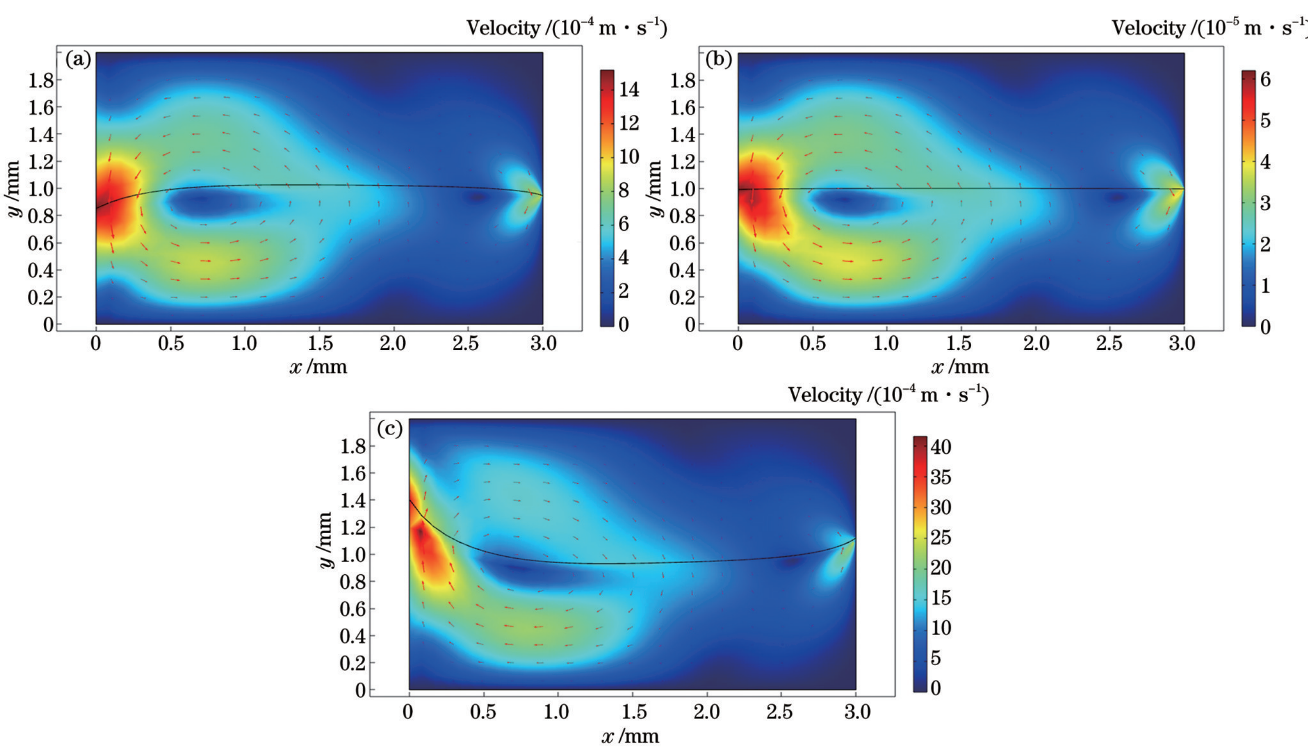


图4 不同电压下COMSOL仿真图。(a) $U$=0 V;(b) $U$=35 V;(c) $U$=60 V

Fig. 4 COMSOL simulation results under different voltages. (a) $U$=0 V; (b) $U$=35 V; (c) $U$=60 V

时，液体透镜界面面型经由凸到平再到凹，当电压到达 60 V 时达到饱和，液体透镜界面不再发生变化。

根据 COMSOL 的仿真结果，利用 MATLAB 软件模拟电压与焦距的关系，得到图 5 所示外部电压与液体透镜焦距之间的关系曲线。从曲线可以看出，当施加电压 0～35 V 时，液体透镜为凸透镜，透镜焦距为[18 mm，+∞)，最终界面变为平面；当施加电压 35～60 V 时，液体透镜为凹透镜，透镜焦距为(−∞，−7.79 mm]，最终达到饱和；当施加 60 V 以上电压时，液体透镜界面不再变化，焦距不再发生改变。

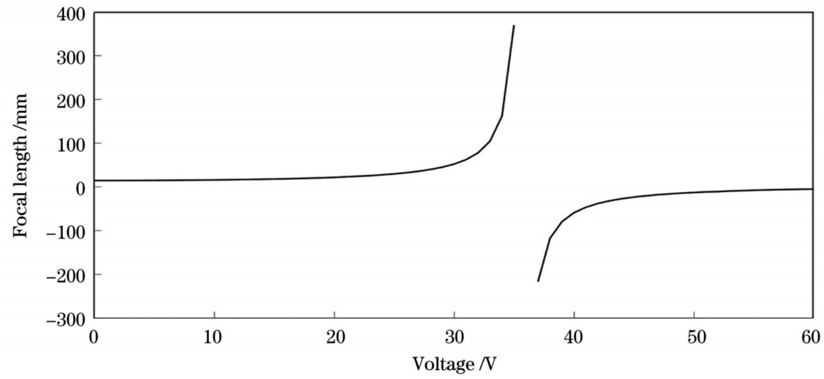


图 5 外部电压与液体透镜焦距的关系

Fig. 5 Relation between external voltage and focal length of liquid lens

### 3.4 液体透镜变焦系统优化及设计结果

将初始结构中变倍组与补偿组替换为液体透镜，通过电压控制液面面型以到达变焦目的。液体透镜变焦系统初始结构如图 6 所示。

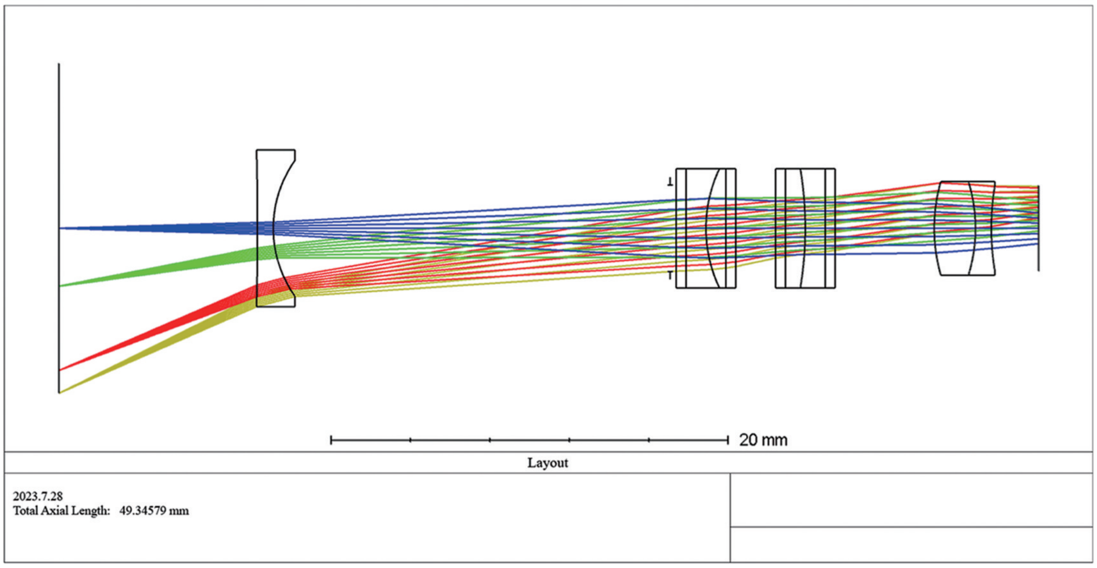


图 6 液体透镜变焦系统初始结构

Fig. 6 Initial structure of liquid lens zoom system

由于液体透镜本身不具备校正像差的能力，因此需要添加透镜来平衡像差。在第一块液体透镜前添加镜组分担光焦度，在减小系统球差的同时使光会聚到液体透镜上；重新设置光阑位置，使系统接近对称结构，以减小畸变、改善慧差；改变两块液体透镜前保护玻璃的光焦度，分担光焦度的同时辅助消色差。在多重结构编辑器中，对不同组态下的参数进行设置，在优化时进行口径限制，对畸变及其他主要像差进行约束，以保证系统成像质量。

优化后变焦镜头结构如图 7 所示，包括短焦(5 mm)、中焦(7.2 mm 和 10.4 mm)、长焦(15 mm)共 4 种状态下的系统结构图。该光学系统第 4 片、第 11 片镜子为液体透镜，在 4 个组态下液体透镜 1 和液体透镜 2 的焦距分别为(−17.89 mm，20.88 mm)、(−48.68 mm，37.43 mm)、(180.73 mm，−631.96 mm)、(38.78 mm，−23.31 mm)，通过 19.44～44.23 V 的电压调节，实现焦距 5～15 mm 的变焦，系统总长度为 45 mm，具体结构参数如表 2 所示，设计好的系统参数如表 3 所示。变焦系统各组态均在最大视场处取得 RMS 半径最大值，最大值均小于像元尺寸 7.4 μm。

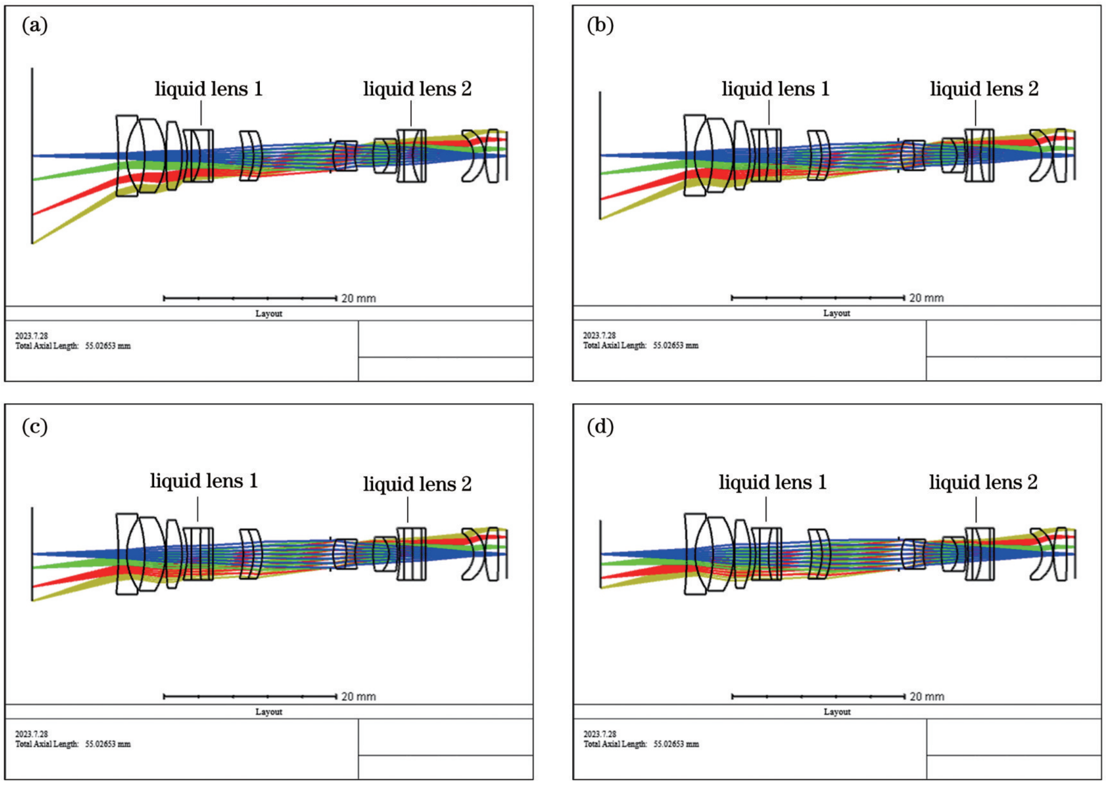


图 7　液体透镜变焦系统结构图。(a)焦距 5 mm；(b)焦距 7.2 mm；(c)焦距 10.4 mm；(d)焦距 15 mm

Fig. 7　Structure of liquid lens zoom system. (a) EFL 5 mm; (b) EFL 7.2 mm; (c) EFL 10.4 mm; (d) EFL 15 mm

表 2　结构参数

Table 2　Structure parameters

| Surface | Radius /mm | Thickness /mm | Material |
|---|---|---|---|
| 1 | Infinity | 10.000 | |
| 2 | −45.898 | 0.980 | H-ZBAF16 |
| 3 | 7.027 | 2.069 | |
| 4 | −13.737 | 2.410 | D-LAK52 |
| 5 | −8.091 | 0.086 | |
| 6 | 48.217 | 1.835 | H-ZLAF50E |
| 7 | −10.645 | 0.600 | |
| 8 | −9.675 | 0.500 | H-ZF73 |
| 9 | Infinity | 1.000 | Sodium chloride solution |
| 10 | Short EFL (5 mm) −5.726, middle EFL (7.2 mm) −15.576, middle EFL (10.4 mm) 57.832, long EFL (15 mm) 12.410 | 1.000 | Silicone oil |
| 11 | Infinity | 0.500 | H-ZK14 |
| 12 | Infinity | 3.496 | |
| 13 | −9.589 | 1.201 | H-K3 |
| 14 | −6.563 | 0.991 | H-ZK10 |
| 15 | −6.972 | 7.935 | |
| 16 | Infinity | 0.299 | |
| 17 | 4.162 | 1.530 | ZF7L |
| 18 | −6.879 | 0.983 | H-ZLAF4LB |
| 19 | 4.658 | 2.106 | |
| 20 | 7.539 | 1.850 | H-LAK52 |

续表

| Surface | Radius /mm | Thickness /mm | Material |
|---|---|---|---|
| 21 | −2.897 | 0.953 | H-ZF73 |
| 22 | −13.700 | 0.295 | |
| 23 | −14.580 | 0.500 | H-BAK7A |
| 24 | Infinity | 1.000 | Sodium chloride solution |
| 25 | Short EFL (5 mm) 6.583, middle EFL (7.2 mm) 11.978, middle EFL (10.4 mm) −202.228, long EFL (15 mm) −7.458 | 1.000 | Silicone oil |
| 26 | Infinity | 0.500 | D-ZLAF52LA-25 |
| 27 | Infinity | 5.550 | |
| 28 | −2.969 | 1.278 | D-LAK70 |
| 29 | −3.577 | 0.086 | |
| 30 | 11.031 | 1.512 | F2 |
| 31 | −47.507 | 0.981 | |

表3 系统参数

Table 3 System parameters

| Focal length /mm | 5 | 7.2 | 10.4 | 15 |
|---|---|---|---|---|
| Field angle /(°) | 22.320 | 32.276 | 45.240 | 61.928 |
| $F^{\#}$ | 5.0 | 5.5 | 6.0 | 6.5 |
| Maximum RMS radius /μm | 4.596 | 3.611 | 4.686 | 6.694 |
| Total length /mm | 45 | 45 | 45 | 45 |

## 4 变焦光学系统成像质量评价

MTF是对镜头分辨率及镜头成像清晰度的定量描述，是像质评价的重要指标。不同组态的光学传递函数（OTF）曲线如图8所示，其中图8(a)～图8(d)分别为焦距为5、7.2、10.4、15 mm时的MTF曲线。由图8可知，在68 lp/mm处，变焦范围内光学系统全视场MTF大于0.5，且接近衍射极限，满足腹腔镜对光学系统的高质量要求。

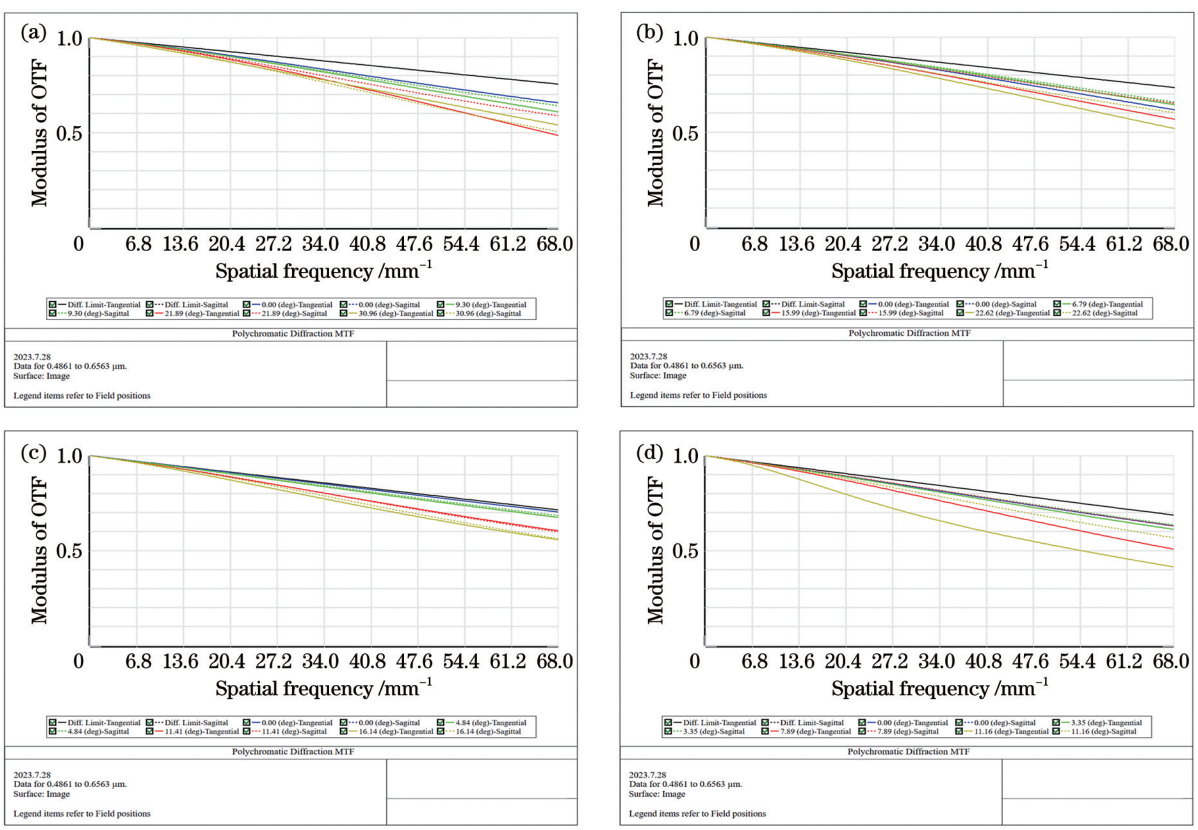


图8 不同焦距MTF图。(a)焦距5 mm；(b)焦距7.2 mm；(c)焦距10.4 mm；(d)焦距15 mm

Fig. 8 MTF curves for different focal lengths. (a) EFL 5 mm; (b) EFL 7.2 mm; (c) EFL 10.4 mm; (d) EFL 15 mm

系统的场曲畸变如图 9 所示，变焦系统在焦距 $f'=15$ mm 时，最大畸变值为 0.295%，在焦距 $f'=10.4$ mm 时，最大畸变值为 0.732%，在焦距 $f'=7.2$ mm 时，最大畸变值为 1.961%，在焦距 $f'=5$ mm 时，最大畸变值为 7.047%，除短焦 5 mm 时畸变略大以外，其余组态畸变均远远小于要求值，对比定焦腹腔镜系统，畸变远小于普遍值 15%，系统性能优异。

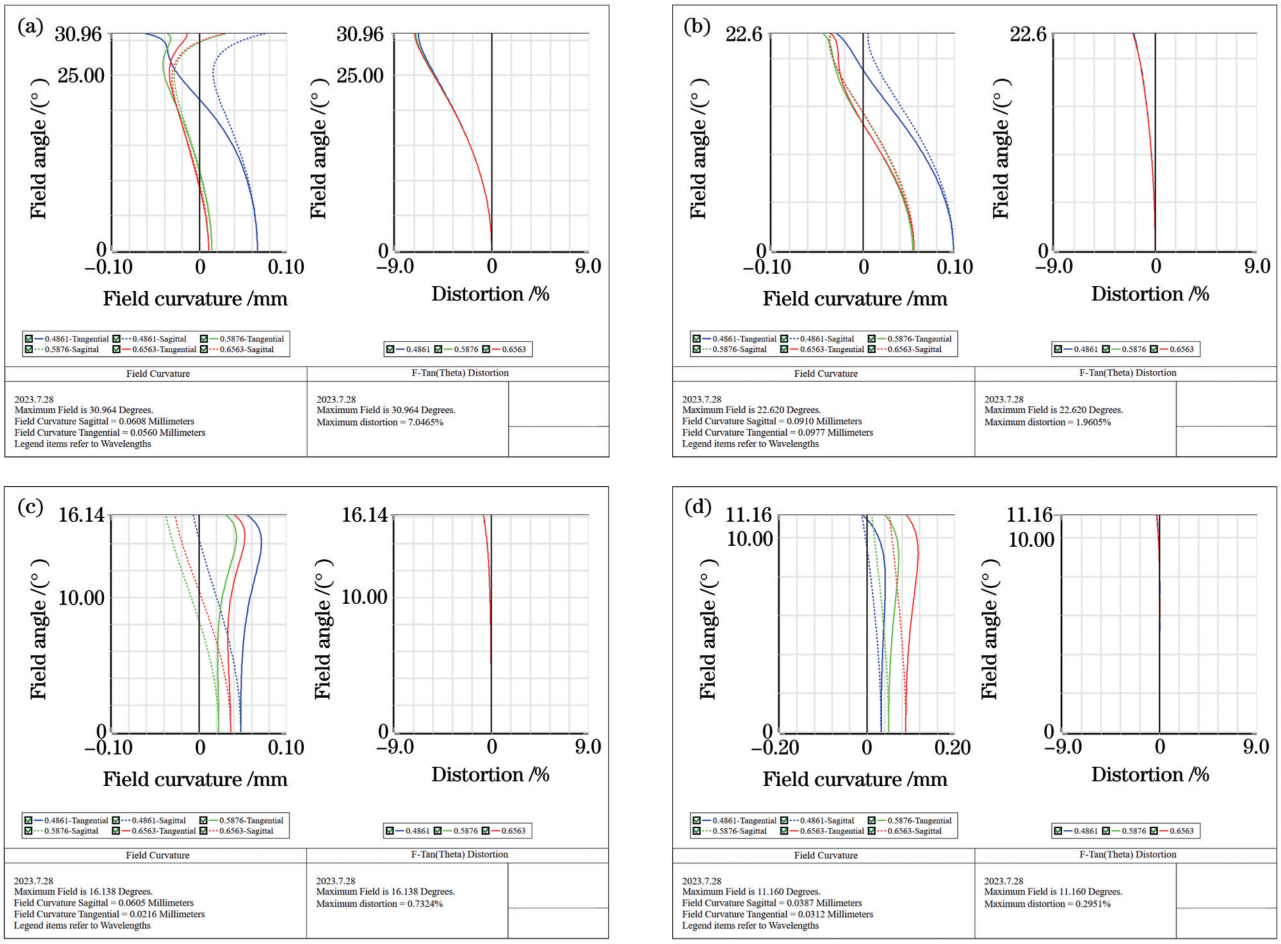


图 9　不同焦距场曲畸变图。(a)焦距 5 mm；(b)焦距 7.2 mm；(c)焦距 10.4 mm；(d)焦距 15 mm

Fig. 9　Field curvature/distortion for different focal lengths. (a) EFL 5 mm; (b) EFL 7.2 mm; (c) EFL 10.4 mm; (d) EFL 15 mm

## 5　结　　论

以液体透镜为核心部件设计了腹腔镜用变焦光学系统，设计并仿真了变焦范围与控制电压的关系。对设计结果进行了像差分析，结果表明 4 个组态 MTF 在奈奎斯特频率 68 lp/mm 处均大于 0.5，最大畸变为 7.047%，成像质量可满足腹腔镜对光学系统畸变的要求。在焦距变化过程中，像面位置始终不变，无需机械结构参与，仅通过调节电压即可实现变焦。设计结果表明利用液体透镜实现腹腔镜变焦光学系统设计是可行的。该方案在减小腹腔镜整体尺寸、提高操作方便性及提高成像质量方面具有广阔的前景。

## 参 考 文 献


[1] Brabcova Z, McHale G, Wells G G, et al. Electric field induced reversible spreading of droplets into films on lubricant impregnated surfaces[J]. Applied Physics Letters, 2017, 110(12): 121603.

[2] Gao J, Mendel N, Dey R, et al. Contact angle hysteresis and oil film lubrication in electrowetting with two immiscible liquids[J]. Applied Physics Letters, 2018, 112(20): 203703.

[3] Davoust L, da Cruz C A, Theisen J. On the use of AC electrowetting for biosensing based on dynamic contact angle[J]. Sensors and Actuators B: Chemical, 2016, 236: 849-857.

[4] 刘永明，谢军，李湘勤，等．弹性薄膜液体透镜的优化设计及面形分析[J]．中国激光，2013，40(12)：1216001.
Liu Y M, Xie J, Li X Q, et al. Optimization and figure analysis of elastic thin-film liquid lens[J]. Chinese Journal of Lasers, 2013, 40(12): 1216001.

[5] Klarman D, Andelman D, Urbakh M. A model of electrowetting, reversed electrowetting, and contact angle saturation[J]. Langmuir, 2011, 27(10): 6031-6041.

[6] Zhang W, Jin Y T, Guo X, et al. Design of an autofocus capsule endoscope system and the corresponding 3D reconstruction algorithm[J]. Journal of the Optical Society of America A, 2016, 33(10): 1970-1977.

[7] 张薇，田维坚，张宏建．二元变焦内窥镜光学系统设计[J]．光子学报，2010，39(1)：105-109.
Zhang W, Tian W J, Zhang H J. A method of bifocal zoom endoscope system design[J]. Acta Photonica Sinica, 2010, 39(1):

105-109.

[8] Tsai F S, Johnson D, Francis C S, et al. Fluidic lens laparoscopic zoom camera for minimally invasive surgery[J]. Journal of Biomedical Optics, 2010, 15(3): 030504.

[9] Lee S, Choi M, Lee E, et al. Zoom lens design using liquid lens for laparoscope[J]. Optics Express, 2013, 21(2): 1751-1761.

[10] 郭鑫，张薇，速晋辉，等．可调焦胶囊内窥镜光学系统设计[J]. 光子学报，2015，44(5): 0522004.
Guo X, Zhang W, Su J H, et al. Design of a focus-tunable capsule endoscope system[J]. Acta Photonica Sinica, 2015, 44(5): 0522004.

[11] Berge B, Peseux J. Variable focal lens controlled by an external voltage: an application of electrowetting[J]. The European Physical Journal E, 2000, 3(2): 159-163.

[12] Mishra K, Murade C, Carreel B, et al. Optofluidic lens with tunable focal length and asphericity[J]. Scientific Reports, 2014, 4: 6378.

[13] Högnadóttir S, Kristinsson K, Thormar H G, et al. Increased droplet coalescence using electrowetting on dielectric (EWOD)[J]. Applied Physics Letters, 2020, 116(7): 073702.

[14] Du K, Cheng X M. Current trends of liquid lenses[C]// International Photonics and OptoElectronics Meetings, June 18-21, 2014, Wuhan, China. Washington, D.C.: Optica Publishing Group, 2014: OF3A.3.

[15] 徐荣青，李雷，孔梅梅，等．电润湿液体透镜暂态过程的测试与分析[J]. 光学学报，2023，43(10): 1023001.
Xu R Q, Li L, Kong M M, et al. Measurement and analysis of transient process of electrowetting liquid lens[J]. Acta Optica Sinica, 2023, 43(10): 1023001.

[16] 绳金侠，彭润玲，陈家璧．电湿效应双液体变焦透镜性能的分析[J]. 光学仪器，2007,29(4): 23-26.
Sheng J X, Peng R L, Chen J B. Analysis on properties of the double-liquid zoom lens based on electrowetting[J]. Optical Instruments, 2007,29(4): 23-26.

[17] Kuiper S, Hendriks B H W. Variable-focus liquid lens for miniature cameras[J]. Applied Physics Letters, 2004, 85(7): 1128-1130.

[18] 赵瑞，马建权，党智勇，等．基于介电润湿三液体透镜的变焦光学系统的设计与分析[J]. 光子学报，2017，46(6): 0622005.
Zhao R, Ma J Q, Dang Z Y, et al. Design and analysis of an optical zoom system using electrowetting-based triple liquid lens[J]. Acta Photonica Sinica, 2017, 46(6): 0622005.

[19] 徐荣青，孔梅梅，张宏超，等．减少电润湿液体透镜变焦时间的实验研究[J]. 光学学报，2020，40(13): 1322003.
Xu R Q, Kong M M, Zhang H C, et al. Experimental research on reducing zoom time of electrowetting liquid lenses[J]. Acta Optica Sinica, 2020, 40(13): 1322003.

[20] Optical Research Associates. CODE V 9.5 introductory user's guide[M]. Pasadena: Optical Research Associates, 2004.

# Design and Study of Liquid Lens Zoom Optical System for Laparoscopy

Dong Jian, Wang Chunyan*, Sun Hao, Liu Huan, Teng Yunjie

*School of Optoelectronic Engineering, Changchun University of Science and Technology, Changchun* 130022, *Jilin, China*

## Abstract

**Objective** At present, the medical endoscope mainly uses the fixed focus optical system and relies on image processing and other means to scale the image. Due to the large space occupied by traditional mechanical zoom optical system as well as its difficulty in zooming, it has not been applied to medical endoscopes. Based on the concept of bionics, the liquid lens is a small, integrated and self-zooming lens. The electrowetting liquid lens is applied to the design of medical endoscope. Zooming can be realized by adjusting the voltage and the image quality can be guaranteed. Some scholars at home and abroad have studied the optical system of endoscope containing liquid lens, but there are many problems in the existing research contents, such as large distortion and difficulty to guarantee the image quality. In this paper, based on the traditional zoom optical design of medical laparoscope, an autonomous zoom optical system with small distortion and simple structure is designed, which is suitable for medical endoscope.

**Methods** The electrowetting liquid lens, which depends on voltage to adjust the curvature of the interface, is selected as the core zoom element. The basic parameters of the optical system are determined according to the main technical indexes, the mechanical zoom optical system is designed by optimizing the initial structure of traditional zoom optics, and the initial optical structure of a zoom laparoscope is obtained. The parameters of liquid lens are determined according to the changing range of focal length and the aperture of optical system, and then the liquid lens is designed and simulated by COMSOL. The simulation diagram of liquid lens interface is given when the voltage is 0, 35 and 60 V. The corresponding relationship between voltage variation and liquid level variation is simulated. When the voltage reaches 60 V, the contact angle of the electrowetting liquid lens reaches saturation, and the liquid lens interface no longer changes. MATLAB software is used to simulate the corresponding relationship between voltage and focal length. In the voltage range of 0–30 V, the focal length is positive and shows a slow growth trend; in the voltage range of 30–35 V, the focal length increases rapidly and finally reaches infinity; when the voltage is in the 35–40 V range, the focal length is negative and rapidly decays from infinity; when the voltage is in the 40–60 V range, the focal length slowly decays, and finally the contact angle of the liquid lens reaches saturation, and the focal length of the liquid lens no longer changes. According to the data, the liquid lens is modeled in ZEMAX. The zoom lens group and compensation lens group in the initial structure are replaced with liquid lenses, and the liquid surface is controlled by voltage to achieve the purpose of zooming. ZEMAX is used to optimize the simulation.

**Results and Discussions** After optimization, the liquid lens zoom optical system for laparoscopy is obtained (Fig. 7), in which the system structure diagrams under four different states are given: short focus (5 mm), medium focus (7.2 mm), medium focus (10.4 mm), and long focus (15 mm), respectively. The fourth and eleventh mirrors of the optical system are liquid lenses. In the four configurations, the focal lengths of liquid lens 1 and liquid lens 2 are (−17.89 mm, 20.88 mm), (−48.68 mm, 37.43 mm), (180.73 mm, −631.96 mm), (38.78 mm, −23.31 mm), respectively. Through 19.44–44.23 V voltage regulation, the focal length of 5–15 mm is realized, and the total length of the system is 45 mm (Table 3). Each state of the zoom system obtains the maximum root-mean-square (RMS) radius at the maximum field angle (Table 3), and all of them are smaller than the pixel size 7.4 μm. The optical transfer function curves of different configurations are all close to the diffraction limit curve (Fig. 8). At the Nyquist frequency of 68 lp/mm, the modulation transfer function (MTF) of the optical system in the zoom range is greater than 0.5, which meets the high quality requirements of the optical system of laparoscopy. The distortion value of each state of the zoom system is far less than the required value, and the maximum distortion value is 7.047% (Fig. 9). Compared with the fixed-focus laparoscopic system, the distortion value is far less than the common value of 15%, showing excellent system performance.

**Conclusions** A zoom optical system for laparoscopy is designed with liquid lens as the core component, and the relationship between zoom range and control voltage is designed and simulated. Aberration analysis of the design results shows that the MTF of the four configurations is greater than 0.5 at the Nyquist frequency of 68 lp/mm, and the maximum distortion is 7.047%. The imaging quality can meet the requirements of laparoscopic optical system. In the process of focal length change, the position of the image plane is always unchanged, and the zooming can be realized by adjusting the voltage without mechanical structure. The results show that it is feasible to use liquid lens to realize the design of laparoscopic zoom optical system. It has a broad application prospect in reducing the overall size, realizing convenient operation and improving the image quality of laparoscopy.

**Key words** optical design; zoom system; liquid lens; laparoscope; COMSOL; ZEMAX